An Efficient TCS Formula for Rainfall Microwave Attenuation: T-Matrix Approach and 3-D Fitting for Oblate Spheroidal Raindrops

Yong-Lee Seow, *Student Member, IEEE*, Le-Wei Li, *Senior Member, IEEE*, Mook-Seng Leong, *Member, IEEE*, Pang-Shyan Kooi, *Member, IEEE*, and Tat-Soon Yeo, *Senior Member, IEEE*

***Abstract*—The T-Matrix approach toward the computation of total cross sections of spheroidal raindrops due to electromagnetic scattering is considered numerically exact, and has therefore been used in this paper for the analysis of the *t*otal *c*ross *s*ection (TCS) of the spheroidal raindrops. A more accurate computer programme based on the T-Matrix method has been developed in MATHEMATICA™ so as to evaluate the TCS's of the spheroidal raindrop scatterers. With the checked programme after comparison, a large amount of TCS data has been obtained and plotted in a three-dimensional (3-D) graphic in this paper. Utilizing these exact data points, a 3-D (or two-step) nonlinear least squares fitting procedure has been proposed and implemented successfully. As a result, an efficient formula of the TCS as a function of both raindrop mean radius and operating frequency has been obtained. In the analysis, four cases (both parallel and perpendicular polarizations, and outdoor temperatures of 10 and 20 °C) are considered. Covering a very large validity range for practical useful problems, this formula is very compact, easy to use, and very much faster (by about two orders of magnitude) than the conventional algorithm.**

***Index Terms*—Electromagnetic scattering, numerical analysis, rainfall attenuation, and radio wave propagation.**

I. INTRODUCTION

OVER the past many years, scattering of plane electromagnetic (EM) waves by various types of scatterers has received much attention in the literature. An exact formulation of scattering of EM waves by perfectly conducting obstacles was given in 1949 by Maue [1], who obtained a pure integral equation which sufficed for the determination of the unknown surface currents on the obstacle. Based on the concept of extended boundary condition, which leads to an extended integral equation where the unknown surface current appears in an integral over the surface, Waterman [2]–[4] proposed a matrix formulation method for the analysis of scattering of plane EM waves by a perfectly conducting obstacle. The matrix formulation method, commonly known as the T-Matrix approach, is both numerically exact and applicable to scatterers of arbitrary shapes and sizes. This matrix formulation method was then further extended by Peterson and Strom [5] to the EM wave scattering by multilayered structures and applied by Barber *et al.* to analyze EM wave scatterings by various dielectric bodies [6]–[10]. Based on the T-Matrix approach, Barber [6] came up with some detailed and simplified theoretical equations easier and more suitable for computer implementation for the case of dielectric scatterers. A computer program written in Fortran language was also developed by Barber [11] which made use of approximations for Bessel and Hankel functions.

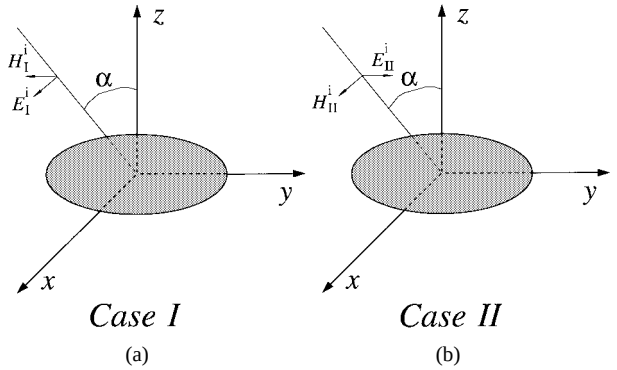

Fig. 1. Geometry of the spheriodal raindrop illuminated by E_x^i and E_y^i polarized plane waves.

The EM scattering by raindrop scatterers has also received much attention in the past many years [12], [13]. The knowledge of microwave rainfall attenuation due to the raindrop scattering is quite important for scientists and engineers in many of their applications. Fig. 1 shows the geometry of a spheroidal raindrop. Among the work published in the literature, the original and most significant contributions with wide recognition has been made first by Oguchi [14], [15] using point-matching techniques and thereafter by Morrison and Cross [16] using the least-squares fitting process of the boundary conditions. The other contributions in this topic are mainly from Erma [17]–[19], who applied sphere-based Taylor expansion to the scattering, Pruppacher and Pitter [20], [21] who developed the "hamburger-shaped" raindrop model known as the P–P model, Asano and Yamamoto [22], who applied spheroidal vector wave function expansion to the scattering, Warner [23], [24], who considered the effects of spheroidal raindrop shape and orientation, Holt *et al.* [25], who applied an integral equation technique in the analysis, and Li *et al.* [26]–[28], who formulated the total cross section and specific attenuation of the "hamburger-shaped" P-P model.

Manuscript received July 2, 1997; revised December 29, 1997. This work was supported in part by a grant under the MINDEF/NUS Joint Project 13/96.

The authors are with the Communications & Microwave Division, Department of Electrical Engineering, National University of Singapore, Singapore 119260.

Publisher Item Identifier S 0018-926X(98)06308-X.

0018–926X/98$10.00 © 1998 IEEE

Since the spheroid is widely adopted as the shape of the raindrops, we will analyze the total cross sections of spheroidal raindrops. The T-Matrix approach leads to an exact analysis and has therefore been applied in the computation of the TCS's of the spheroidal raindrops. We have tried a couple of computer programs written in Fortran based on an approximated form of spherical Bessel and Hankel functions. However, it is found that such programs do not work well (or accurately) when the raindrop size or the operating frequency becomes large (mainly due to the approximations of the Bessel and Hankel functions after detailed check).

As the Mathematica™ package is an accurate commercial software with very good symbolic and numerical functions and has been used widely, we have rewritten the T-Matrix program using exact Bessel and Hankel equations to cater directly to the application of spheroidal raindrop scatterers in the Mathematica™ programming language. As the method applied is exactly the same as that introduced by [6] and [11], no details will be provided in this paper. Instead, we would present a large number of data points of the TCS's of the spheroidal raindrops for the scientists or engineers to use. These data points are given in terms of a three-dimensional (3-D) figure instead of being tabulated in a large number of tables. The tabulated data are readily available in [29] and can be supplied upon request.

However, for more efficient utilization of these readily available data of the TCS of spheroidal raindrops, we have developed a 3-D (or two-step) curve-fitting procedure with Mathematica™ program. An efficient and compact formula as a function of both raindrop mean radius a_0 (cm) and operating frequency f (GHz) has been successfully obtained for each of the four cases, i.e., parallel and perpendicular incident polarizations, and temperatures of 10 and 20 °C.

The theoretical fundamentals for the computer program implementation can be found in [2], and hence will not be given for the problem where the geometry of EM scattering by a spheroidal raindrop is shown in Fig. 1 in Section I. Section II briefly addresses the mathematical expression of the oblate spheroidal raindrops, the comparison of the currently generated exact data and those published results using other methods, and the validation coverage of the developed formula using a 3-D least-squares fitting process. In Section III, the curve-fitting procedure is detailed and subsequently the resulting formula together with its coefficients are tabulated in a table. Error analysis of the fitting process is carried out in Section IV and comparisons are also made between the exact results computed using the T-Matrix Approach and the fitted results applying the 3-D nonlinear least-squares fitting procedure.

II. Spheroidal Raindrop Shape and Data Generation

The raindrops scattering analysis has been carried out using the oblate spheroidal model shown in Fig. 1.

A. Oblate Shape Expression

The $\hat{z}$-direction is considered as the axis of revolution and the incident EM illumination is characterized here by the E-field component normal to this axis. In other words, a parallel polarized incident field is characterized by the field component $\boldsymbol{E}_x^i$ and a perpendicular polarized incident field by the component $\boldsymbol{E}_y^i$; see Fig. 1. In the coordinate system of this figure, the equation describing the spheroidal raindrop shape is given as follows:

$$r(\theta) = \frac{a_0(1-a_0)^{2/3}}{\sqrt{1-a_0(2-a_0)\cos^2(\theta)}} \tag{1}$$

where a_0 (in centimeters) stands for the input raindrop mean radius introduced earlier by Laws and Parsons [30] and Oguchi [12].

The relative dielectric constant $\epsilon(f,T)$ of the raindrop is dependent upon the operating frequency f (GHz) and the outdoor temperature T (°C). In this work, the corresponding refractive index has been computed using the Ray's program [31] written in Fortran language.

B. Comparison of Results and Correctness of Programming

Using the computer program developed, various values for the TCS's of spheroidal raindrops illuminated by a EM plane wave of unit amplitude have been generated and compared to those values provided by Morrison and Cross [16] who employed the least-squares fitting technique to the spheroidal raindrops' boundary conditions.

To ensure the correctness of the program, a two-step examination has been taken. First, the T-Matrix program has been verified by comparing the results of the TCS's for spherical raindrops that were generated using the T-Matrix program and the Mie scattering algorithm. The comparison shows that the two sets of results were in very good agreement with a deviation of less than 1.5%, as expected. Secondly, the TCS values at the frequencies of 11, 18.1 and 30 GHz at a temperature of 20 °C (i.e., the same conditions assumed by Morrison and Cross [16]) have also been generated and compared with those in [16]. The values generated by the two methods also agree very well and deviate by a relative error of less than 2%. Based on these comparisons with available published data, the validity of the new program developed here is confirmed.

C. Data Generation and Presentation

Once the computer program had been verified to work perfectly, a large number of data points of TCS's against the oblate spheroidal raindrop mean radius a_0 (cm) and the operating frequency f (GHz) have been generated. As indicated earlier, both parallel and perpendicular incident polarizations and two outdoor temperatures (i.e., 10 and 20 °C) have been taken into account in the data generation using the newly developed T-Matrix computer program. It shows that the TCS increases as frequency is increased for parallel polarization, but is decreased for perpendicular polarization direction as $a > 2.5$ mm.

III. Curve Fitting and Formula Generation

Based on the exact data generated using the T-Matrix Method, a 3-D curve fitting procedure has been conducted over

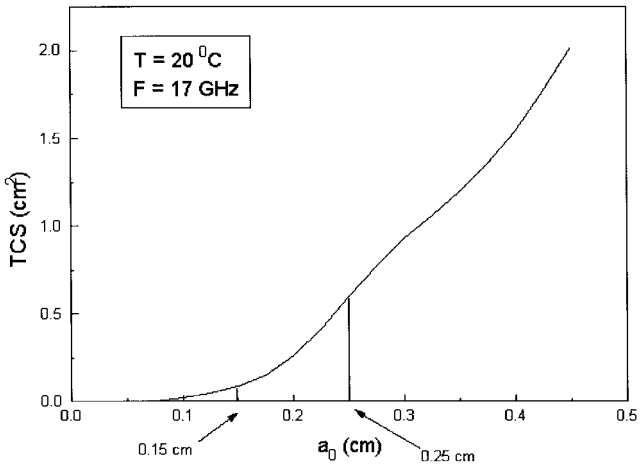

Fig. 2. Break points for the TCS versus a_0 curve. The curve shown is that for a EM wave of parallel incident polarization on spheroidal raindrops at temperature of 20 °C and frequency at 17 GHz.

different ranges of raindrop mean radius a_0 (cm), operating frequency f (GHz) and outdoor temperatures T (°C). However, as the one-step commercial nonlinear 3-D least squares fitting package is not readily available, we used a two-step two-dimensional (2-D) fitting procedure in the 3-D fitting. First, the graphs of TCS (Q_t) against mean radius a_0 were fitted with suitable curves which will be discussed in greater detail later. Next the coefficients of these well-fitted curves were again fitted against operating frequency. The same process is applied at both temperatures of 10 and 20 °C and for both parallel and perpendicular incident polarizations.

A. Fitting I: TCS Versus Mean Radius

It has been realized after many tests that a single function cannot give a good fitting of the TCS (within the given frequency range 10–80 GHz) against the mean radius a_0 at a given temperature. After observing the curves of TCS's against a_0 for all ranges of frequency and temperature, it was decided to break the curves into three sections, each fitted with a different equation and ensuring continuity at joining points. After trying out various approaches for the three separate fitting sections, we chose the break points 0.15 and 0.25 cm as a good compromise between minimizing the number of sections and obtaining a good fit. To gain insight into the detailed variation, Fig. 2 shows the TCS (cm^2) against the raindrop mean radius a_0 (cm) and the two proposed break points.

The equations for the different mean radius sections were selected as follows:

$$Q_t(a_0) = \begin{cases} a_0(C_0 + C_1 a_0)^2, & 0.00 \le a_0 \le 0.15 \\ C_2 + C_3 a_0 + C_4 a_0^2 + C_5 a_0^3, & 0.15 \le a_0 \le 0.25 \\ C_6 + C_7 a_0 + C_8 a_0^2 + C_9 a_0^3, & 0.25 \le a_0 \le 0.45 \end{cases} \tag{2}$$

where $Q_t(a_0)$ is the total cross section at a mean radius a_0 (cm) and C_0 to C_9 in (2) are the ten unknown coefficients that need to be determined.

After trying out various other equations such as exponential and second-degree polynomials which were not satisfactory, we found that the third-degree polynomials can lead to very good fittings and they have therefore been chosen. The equations selected must be able to fit across all frequencies within 10–80 GHz and temperatures 10 and 20 °C to a good extent of about 5% relative error. Using the selected equations, there were ten unknown coefficients to be determined over the range of a_0 up to 0.45 cm.

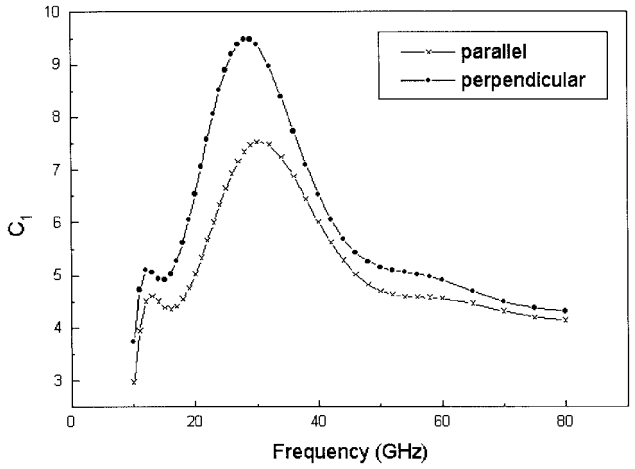

(a)

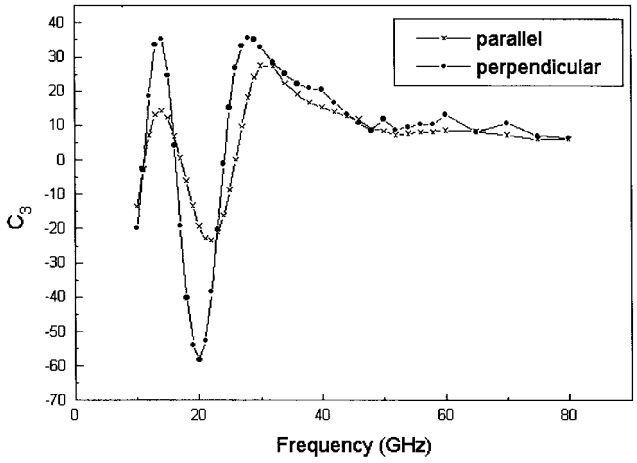

(b)

Fig. 3. Graphs of coefficients, C_1 and C_3 as examples, versus the frequency f (GHz). The coefficients shown have obtained for the case of spheroidal raindrops at temperature of 20 °C illuminated by a unit amplitude plane EM wave of parallel incident polarization.

B. Fitting II: Coefficients Versus Frequency

To determine the ten coefficients in (2) for frequencies ranging from 10 to 80 GHz (in steps of 1 GHz), the coefficients, C_0 to C_9 for both parallel (E_x^i) and perpendicular (E_y^i) incident polarizations and at a temperature of 20 °C, have been plotted against frequency in an attempt to perform the second round of curve fitting or the 3-D fitting. Two examples are shown in Fig. 3(a) and (b) for coefficients C_1 and C_3. At a temperature of 10 °C, similar graphs have been obtained (except with different degree of fluctuation across the higher frequency region) but will not be given here to save space.

TABLE I
FORMULA AND ITS COEFFICIENTS FOR BOTH E_x^i AND E_y^i POLARIZATIONS AT BOTH 10 AND 20 °C

Cases			Raindrip Mean Radius Ranges					
	T	f	0 cm $\le a_0 \le$ 0.15 cm		0.15 cm $\le a_0 \le$ 0.25 cm		0.25 cm $\le a_0 \le$ 0.45 cm	
			$Q_t(a_0) = a_0(C_0 + C_1 a_0)^2$	Err	$Q_t(a_0) = C_2 + C_3 a_0 + C_4 a_0^2 + C_5 a_0^3$	Err	$Q_t(a_0) = C_6 + C_7 a_0 + C_8 a_0^2 + C_9 a_0^3$	Err
E_x^i	10	10	$C_0 = 3.884 - 0.919f + 0.08f^2$	7%	$C_2 = 0.359 + 0.65e^{0.016}f\cos(15.409 + 0.456f)$	5%	$C_6 = -0.277 + 2.22e^{-0.007}f\cos(13.446 + 0.484f)$	5%
		|	$-0.003f^3 + 4.023\times10^{-5}f^4$		$C_3 = -6.453 + 11.308e^{0.017}f\cos(12.394 + 0.447f)$		$C_7 = 1.69 - 23.683e^{-0.017}f\cos(0.685 + 0.488f)$	
		25	$C_1 = -38.156 + 9.541f - 0.804f^2$		$C_4 = 37.967 + 63.6657e^{0.018}f\cos(15.685 + 0.436f)$		$C_8 = 3.66 + 69.546e^{-0.018}f\cos(13.02 + 0.495f)$	
			$+0.03f^3 - 0.0004f^4$		$C_5 = -50.485 - 116.837e^{0.017}f\cos(15.68 + 0.433f)$		$C_9 = -1.929 - 67.452e^{-0.02}f\cos(56.809 + 0.5f)$	
		25	$C_0 = 5.024 - 0.478f + 0.014f^2$	3%	$C_2 = -1.094 - 93.308e^{-0.15}f\cos(21.841 + 0.294f)$	7%	$C_6 = -0.044 - 27.113e^{-0.111}f\cos(17.379 + 0.452f)$	4%
		|	$-1.285\times10^{-4}f^3$		$C_3 = 16.6 + 1641.5e^{-0.154}f\cos(21.404 + 0.309f)$		$C_7 = 0.507 + 247.708e^{-0.113}f\cos(17.137 + 0.458f)$	
		44	$C_1 = -46.646 + 4.654f - 0.128f^2$		$C_4 = -71.761 + 8779.814e^{-0.156}f\cos(11.562 + 0.324f)$		$C_8 = 6.781 + 715.97e^{-0.113}f\cos(20.11 + 0.463f)$	
			$+1.122\times10^{-3}f^3$		$C_5 = 121.118 - 14858.51e^{-0.157}f\cos(1.401 - 0.338f)$		$C_9 = -2.826 + 731.088e^{-0.116}f\cos(35.448 + 0.473f)$	
		44	$C_0 = -1.742 + 0.095f - 0.001f^2$	2%	$C_2 = -13.861 + 0.63f - 0.01f^2 + 5.119\times10^{-5}f^3$	2%	$C_6 = -6.989 + 0.313f - 0.005f^2 + 2.298\times10^{-5}f^3$	3%
		|	$+6.833\times10^{-6}f^3$		$C_3 = 221.853 - 10.134f + 0.159f^2 - 8.241\times10^{-4}f^3$		$C_7 = 54.52 - 2.4f + 0.036f^2 - 1.732\times10^{-4}f^3$	
		80	$C_1 = 20.463 - 0.714f + 0.011f^2$		$C_4 = -1135 + 52.404f - 0.821f^2 + 4.257\times10^{-3}f^3$		$C_8 = -126 + 5.782f - 0.084f^2 + 4.039\times10^{-4}f^3$	
			$-5.513\times10^{-5}f^3$		$C_5 = 1889 - 87.009f + 1.363f^2 - 0.007f^3$		$C_9 = 91.136 - 3.923f + 0.056f^2 - 2.602\times10^{-4}f^3$	
	20	10	$C_0 = 6.666 - 1.642f + 0.145f^2$	7%	$C_2 = 0.390 - 2.278e^{-0.042}f\cos(12.768 + 0.427f)$	5%	$C_6 = -0.232 + 2.803e^{-0.018}f\cos(7.629 + 0.46f)$	5%
		|	$-0.005f^3 + 7.48\times10^{-5}f^4$		$C_3 = -7.114 + 38.198e^{-0.04}f\cos(12.842 + 0.42f)$		$C_7 = 1.398 - 28.168e^{-0.025}f\cos(7.39 + 0.466f)$	
		25	$C_1 = -67.5 + 17.023f - 1.472f^2$		$C_4 = 42.655 - 205.867e^{-0.037}f\cos(12.936 + 0.412f)$		$C_8 = 4.177 + 79.826e^{-0.024}f\cos(13.425 + 0.474f)$	
			$+0.055f^3 - 7.43\times10^{-4}f^4$		$C_5 = -59.769 + 356.623e^{-0.036}f\cos(12.934 + 0.409f)$		$C_9 = -2.382 + 74.514e^{-0.025}f\cos(10.064 + 0.481f)$	
		25	$C_0 = 4.971 - 0.460f + 0.013f^2$	3%	$C_2 = -1.045 + 104.554e^{-0.154}f\cos(18.712 + 0.29f)$	7%	$C_6 = -0.073 - 52.195e^{-0.134}f\cos(17.175 + 0.458f)$	4%
		|	$-1.19\times10^{-4}f^3$		$C_3 = 15.866 - 1894.89e^{-0.159}f\cos(18.265 + 0.305f)$		$C_7 = 0.827 + 504.682e^{-0.138}f\cos(16.830 + 0.468f)$	
		44	$C_1 = -44.954 + 4.398f - 0.119f^2$		$C_4 = -68.423 + 10401.48e^{-0.162}f\cos(1.012 - 0.32f)$		$C_8 = 5.478 + 1546.212e^{-0.141}f\cos(19.705 + 0.476f)$	
			$+1.02\times10^{-3}f^3$		$C_5 = 115.556 - 18075.26e^{-0.164}f\cos(1.42 - 0.335f)$		$C_9 = -1.608 + 1749.89e^{-0.148}f\cos(16.052 + 0.491f)$	
		44	$C_0 = -1.997 + 0.107f - 0.002f^2$	2%	$C_2 = -12.054 + 0.546f - 0.009f^2 + 4.456\times10^{-5}f^3$	2%	$C_6 = -1.497 + 0.054f - 6.666f^2 + 2.782\times10^{-6}f^3$	3%
		|	$+7.87\times10^{-6}f^3$		$C_3 = 188.504 - 8.565f + 0.134f^2 - 7.008\times10^{-4}f^3$		$C_7 = 18.315 - 0.712f + 0.01f^2 - 4.475\times10^{-5}f^3$	
		80	$C_1 = 22.732 - 0.829f + 0.013f^2$		$C_4 = -933.91 + 42.91f - 0.674f^2 + 3.508\times10^{-3}f^3$		$C_8 = -79.154 + 3.711f - 0.054f^2 + 2.649\times10^{-4}f^3$	
			$-6.48\times10^{-5}f^3$		$C_5 = 1505 - 68.837f + 1.081f^2 - 0.006f^3$		$C_9 = 133.039 - 6.193f + 0.095f^2 - 4.778\times10^{-4}f^3$	
E_y^i	10	10	$C_0 = 4.22 - 1.057f + 0.096f^2$	7%	$C_2 = 0.876 + 2.323e^{0.00459}f\cos(15.078 + 0.508f)$	5%	$C_6 = -0.51 + 14.562e^{-0.058}f\cos(6.748 + 0.56f)$	5%
		|	$-0.004f^3 + 5.392\times10^{-5}f^4$		$C_3 = -14.981 + 44.121e^{-0.001}f\cos(18.285 + 0.502f)$		$C_7 = 3.537 - 150.735e^{-0.067}f\cos(0.165 + 0.572f)$	
		25	$C_1 = -41.842 + 11.005f - 0.978f^2$		$C_4 = 81.754 + 277.164e^{-0.007}f\cos(15.223 + 0.495f)$		$C_8 = 1.125 - 464.259e^{-0.071}f\cos(15.623 + 0.582f)$	
			$+0.038f^3 - 5.396\times10^{-4}f^4$		$C_5 = -109.162 + 546.637e^{-0.013}f\cos(18.362 + 0.492f)$		$C_9 = 7.69 + 431.855e^{-0.07}f\cos(53.122 + 0.59f)$	
		25	$C_0 = 6.109 - 0.63f + 0.02f^2$	5%	$C_2 = -0.978 + 4305.077e^{-0.251}f\cos(23.883 + 0.115f)$	7%	$C_6 = -0.072 - 436.174e^{-0.208}f\cos(18.761 + 0.455f)$	6%
		|	$-1.883\times10^{-4}f^3$		$C_3 = 14.577 - 351908e^{-0.286}f\cos(31.516 + 0.06f)$		$C_7 = 0.824 - 4903.038e^{-0.218}f\cos(21.695 + 0.462f)$	
		44	$C_1 = -61.476 + 6.484f - 0.19f^2$		$C_4 = -67.754 + 1000027.9e^{-0.296}f\cos(17.032 + 0.137f)$		$C_8 = 7.321 - 17634.3e^{-0.226}f\cos(18.333 + 0.469f)$	
			$+0.002f^3$		$C_5 = 115.859 + 8375943.1e^{-0.337}f\cos(2.58 + 0.086f)$		$C_9 = -0.395 + 14261.52e^{-0.221}f\cos(37.343 + 0.463f)$	
		44	$C_0 = -0.629 + 0.041f - 5.202$	2%	$C_2 = -2.149 + 0.051f - 5.323\times10^{-4}f^2 + 2.11\times10^{-6}f^3$	2%	$C_6 = 2.347 - 0.173f + 0.0036f^2 - 2.335\times10^{-5}f^3$	3%
		|	$\times10^{-4}f^2 + 2.322\times10^{-6}f^3$		$C_3 = 30.79 - 0.684f + 6.693\times10^{-3}f^2 - 2.417\times10^{-5}f^3$		$C_7 = -22.831 + 1.662f - 0.035f^2 + 2.21\times10^{-4}f^3$	
		80	$C_1 = 11.696 - 0.242f + 0.003f^2$		$C_4 = -135.225 + 3.096f - 0.028f^2 + 8.218\times10^{-5}f^3$		$C_8 = 77.946 - 4.949f + 0.102f^2 - 6.556\times10^{-4}f^3$	
			$-1.337\times10^{-5}f^3$		$C_5 = 225.807 - 4.7f + 0.035f^2 - 6.398\times10^{-5}f^3$		$C_9 = -56.67 + 4.238f - 0.091f^2 + 5.967\times10^{-4}f^3$	
	20	10	$C_0 = 6.064 - 1.574f + 0.146f^2$	7%	$C_2 = 0.836 - 3.275e^{-0.012}f\cos(12.182 + 0.491f)$	5%	$C_6 = -0.49 + 14.902e^{-0.06}f\cos(6.838 + 0.553f)$	5%
		|	$-0.006f^3 + 8.139\times10^{-5}f^4$		$C_3 = -14.358 + 60.239e^{-0.016}f\cos(18.506 + 0.487f)$		$C_7 = 3.367 - 152.954e^{-0.068}f\cos(6.54 + 0.565f)$	
		25	$C_1 = -62.638 + 16.636f - 1.502f^2$		$C_4 = 78.851 + 364.894e^{-0.02}f\cos(15.416 + 0.481f)$		$C_8 = 1.42 + 468.035e^{-0.072}f\cos(12.572 + 0.575f)$	
			$+0.059f^3 - 8.216\times10^{-4}f^4$		$C_5 = -105.24 - 698.239e^{-0.024}f\cos(15.401 + 0.479f)$		$C_9 = 7.38 - 432.8e^{-0.071}f\cos(6.087 + 0.583f)$	
		25	$C_0 = 6.477 - 0.646f + 0.02f^2$	3%	$C_2 = -1.001 - 3701.03e^{-0.248}f\cos(20.622 + 0.118f)$	7%	$C_6 = -0.135 + 99.797e^{-0.157}f\cos(15.202 + 0.469f)$	4%
		|	$-1.86\times10^{-4}f^3$		$C_3 = 15.893 - 95689.234e^{-0.25}f\cos(23.487 + 0.128f)$		$C_7 = 1.425 - 655.545e^{-0.147}f\cos(21.389 + 0.472f)$	
		44	$C_1 = -63.009 + 6.478f - 0.186f^2$		$C_4 = -66.367 + 2604446.9e^{-0.311}f\cos(5.908 + 0.078f)$		$C_8 = 5.293 + 1558.404e^{-0.142}f\cos(52.664 + 0.477f)$	
			$+1.7\times10^{-3}f^3$		$C_5 = 120.1 + 6612950.9e^{-0.336}f\cos(2.227 + 0.099f)$		$C_9 = 1.7 + 2202.73e^{-0.156}f\cos(17.934 + 0.482f)$	
		44	$C_0 = -0.868 + 0.053f - 7.07$	2%	$C_2 = -8.046 + 0.371f - 0.006f^2 + 3.46\times10^{-5}f^3$	2%	$C_6 = -12.82 + 0.665f - 0.012f^2 + 6.468\times10^{-5}f^3$	3%
		|	$\times10^{-4}f^2 + 3.322\times10^{-6}f^3$		$C_3 = 130.068 - 6.088f + 0.103f^2 - 5.737\times10^{-4}f^3$		$C_7 = 120.512 - 6.236f + 0.108f^2 - 6.053\times10^{-4}f^3$	
		80	$C_1 = 13.726 - 0.346f + 0.005f^2$		$C_4 = -675.891 + 32.564f - 0.551f^2 + 0.003f^3$		$C_8 = -370.322 + 19.636f - 0.339f^2 + 1.9\times10^{-3}f^3$	
			$-2.248\times10^{-5}f^3$		$C_5 = 1172 - 56.389f + 0.956f^2 - 0.005f^3$		$C_9 = 408.335 - 21.126f + 0.362f^2 - 0.002f^3$	

Again, it is seen from Fig. 3 that each of these coefficients cannot be well-fitted by using a single function. For a better fitting of these second-step curves, the ten coefficients versus frequency have again been separated into three different frequency sections, i.e., 10–25 GHz, 25–44 GHz, and 44–80 GHz. And correspondingly, the following three types of equations have actually been employed in the fitting process where the subscript i stands for a value between zero and nine for the coefficients C_0 to C_9:

$$C_i = \begin{cases} \alpha_0 + \alpha_1 f + \alpha_2 f^2 + \alpha_3 f^3 + \alpha_4 f^4 \\ \beta_0 + \beta_1 e^{\beta_2 f}\cos[\beta_3 + \beta_4 f] \\ \gamma_0 + \gamma_1 f + \gamma_2 f^2 + \gamma_3 f^3 \end{cases} \tag{3}$$

where the subcoefficients shown in (3)—α_ℓ ($\ell = 0, 1, 2, 3$ and 4), β_ℓ and γ_κ ($\kappa = 0$, 1, 2 and 3)—denote the unknowns to be determined from the second-round least-squares curve-fitting procedure.

Again, the least-squares fitting procedure is applied to the curves obtained from the second round after the completion of the curve fitting in (2). The unknown subcoefficients in (3) are thereafter obtained for different ranges of raindrop mean radius a_0 (cm) and operating frequency f (GHz). They are tabulated in a very compact form in Table I at a temperature T and for a polarization E^i (T, E^i) from (10 °C, 20 °C), (E_x^i, E_y^i). It implies that four cases as shown in Table I have been considered and therefore four sets of the formulas have been obtained.

C. Validation Coverage of the Formula

The formula of TCS's developed using incident field with unit amplitude is applicable for oblate spheroidal raindrops with mean (effective) drop radius ranging up to 0.45 cm and frequency from 10 to 80 GHz because of its corresponding range used for data generation. The validation coverage of both the data readily available and the formula developed has been summarized as follows:

Parameter	Symbol	Range
Mean drop radius	a_0	0.00–0.45 cm
Frequency	f	10-80 GHz
Temperature	T	10 and 20 °C
Polarization	$E_{x,y}^i$	Parallel & Perpendicular

IV. ERROR ANALYSIS AND DATA COMPARISON

Although there are quite a number of coefficients to be determined for any particular set of operating frequencies and

raindrop sizes, the formulas obtained are rather compact. These formulas involve exponential and cosine functions and can be easily calculated. The maximum degree of polynomial is restricted to four and it is mainly used for raindrops at low frequencies and small raindrop mean radii. It should be noted that the general formula for both temperatures of 10 and 20 °C and both parallel and perpendicular polarizations is the same as given in (2) and (3), and only the values of the coefficients vary.

A lot of trials were carried out using different equations and separating the curves at different positions in an effort to come up with the most suitable formula. Due to the wide range of parameters considered, it is very difficult to find equations that fit uniformly across all the parameters. A particular equation might fit values at one frequency perfectly but at the same time causing significant error in the fitting at another frequency.

The curve-fitting procedure in Section III was carried out separately using a two-step approach. The errors introduced in each fitting process therefore cause the overall results to suffer higher errors (7%) at certain frequencies and size regions and at the same time slight discontinuity across the regions (see the relative errors namely "Err" in Table I). Large errors at certain regions can occur and are found basically due to the summation of errors over the two fitting processes, especially at a highly nonlinear region of $0.15 \text{ cm} \leq a_0 \leq 0.25 \text{ cm}$. Particularly, large errors (7%) also occur near 10 GHz due mainly to the fact that the fitting of coefficients in (3) starts at this point, therefore resulting in insufficient information to get a good fit.

The errors can be reduced by considering smaller frequency and size regions. However, it also results in more different formulas to be used. Therefore, the method employed in this work is a compromise between the number of formulas and degree of accuracy.

Although the errors arising from using the formula at certain small regions over the whole 2-D regions are considerable, the fitted formulas are able to provide a rather good estimation of the TCS for oblate spheroidal raindrops. Fig. 4(a) and (b) shows two 2-D plots, respectively, for the parallel and perpendicular polarizations. From the comparison as shown in Fig. 4, it is seen that the two results obtained by using numerically exact T-Matrix Method and applying the least-squares curve fitting formulas generated in this work are in excellent agreement. The relative errors, as expected, are basically acceptable for practical problems.

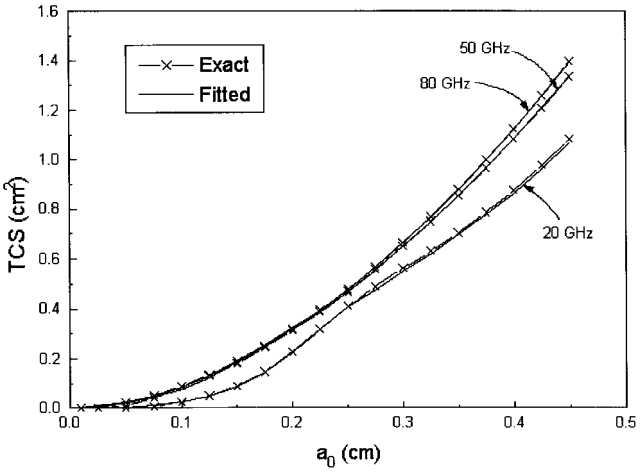

(a)

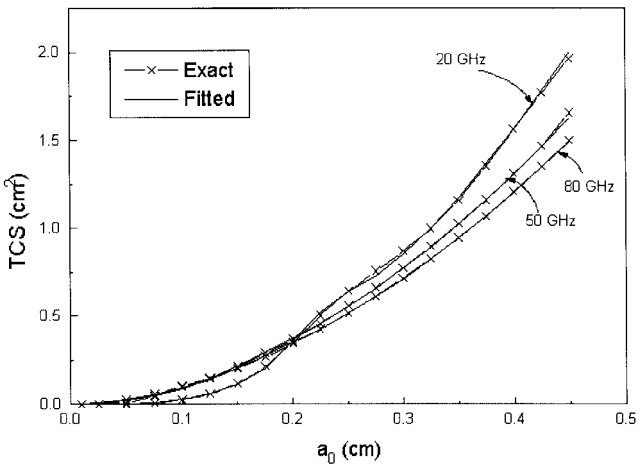

(b)

Fig. 4. Comparison between the results obtained using T-Matrix Method and least-squares curve fitting for TCS's of oblate spheroidal raindrops at a temperature of 20 °C. Both parallel and perpendicular incident polarizations are considered in the analysis of the TCS's at a frequency of 20, 50, and 80 GHz.

V. Conclusion

Based on the T-Matrix Approach developed by Waterman [2] and Barber [6], a more accurate algorithm than that of Baber and/or Hill [6], [11] in Fortran language has been developed with Mathematica™ for evaluating the total cross section of spheroidal raindrops illuminated by a unit amplitude EM wave. By utilizing this more accurate algorithm, a huge number of TCS data against both raindrop mean radius a_0 (cm) and the operating frequency f (GHz) have been generated and plotted.

With these generated data, a very efficient formula for TCS's of oblate spheroidal raindrops has been obtained by applying a 3-D (or two-step) curve-fitting procedure. It is a rather compact formula, consisting of cosine, exponential and polynomial functions. As compared with the T-Matrix algorithm, the computational speed by using this formula is increased by about two orders. This formula is very easy to use because it does not 1) require special functions such as the spherical Bessel functions and associate Legendre functions, and 2) encounter convergence problem and therefore needs no special considerations of the Bessel functions' special properties (when index number and argument are comparable). It covers the practical usable range of raindrop radius (up to 0.45 cm), operating frequency (10–80 GHz), and outdoor temperature (10 and 20 °C), and includes both parallel and perpendicular incident polarizations. Hence, it is a very useful and efficient formula for users to evaluate the total cross section of oblate spheroidal raindrops for microwave rainfall attenuation calculation.

REFERENCES

[1] A. W. Maue, "Formulation of general diffraction problems through an integral equation," *J. Phys.*, vol. 126, pp. 601–618, 1949.

[2] P. C. Waterman, "Matrix formulation of electromagnetic scattering," *Proc. IEEE*, vol. 53, pp. 805–812, 1965.

[3] ——, "Summetry, unitarity, and geometry in electromagnetic scattering," *Phys. Rev. D*, vol. 3, no. 4, pp. 825–839, 1971.

[4] ——, "Matrix methods in potential theory and electromagnetic scattering," *J. Appl. Phys.*, vol. 50, no. 7, pp. 4550–4566, 1979.

[5] B. Perterson and S. Strom, "T-matrix formulation o felectromagnetic scattering from multilayered scatterers," *Phys. Rev. D*, vol. 10, no. 8, pp. 2670–2684, Oct. 1974.

[6] P. W. Barber, "Differential scattering of electromagnetic waves by homogeneous isotropic dielectric bodies," Ph.D. dissertation, Univ. of California, Los Angeles, 1973.

[7] P. W. Barber and C. Yeh, "Scattering of electromagnetic waves by arbitrarily shaped dielectric bodies," *Appl. Opt.*, vol. 14, no. 12, pp. 2864–2872, Dec. 1975.

[8] D. S. Wang and P. W. Barber, "Scattering by inhomogeneous nonspherical objects," *Appl. Opt.*, vol. 18, no. 8, pp. 1190–1197, Apr. 1979.

[9] D. S. Wang, M. Kerker, and H. W. Chew, "Raman and fluorescent scattering by molecules embedded in dielectric spheroids," *Appl. Opt.*, vol. 19, no. 14, pp. 2315–2328, July 1979.

[10] K. C. Yeh and C. H. Liu, "Radio wave scintillation in the ionosphere," *Proc. IEEE*, vol. 70, pp. 324–360, 1982.

[11] P. W. Barber and S. C. Hill, *Light Scattering by Particles: Computational Methods*. Singapore: World Scientific, 1990.

[12] T. Oguchi, "Scattering from hydrometeors: A survey," *Radio Sci.*, vol. 16, pp. 691–730, 1981.

[13] ——, "Electromagnetic wave propagation and scattering in rain and other hydrometeors," *Proc. IEEE*, vol. 71, pp. 1029–1078, 1983.

[14] ——, "Attenuation of electromagnetic wave due to rain with distorted raindrops," *J. Radio Res. Labs.*, vol. 7, pp. 467–485, 1960.

[15] ——, "Attenuation of electromagnetic wave due to rain with distorted raindrops (Part II)," *J. Radio Res. Labs.*, vol. 11, pp. 19–44, 1964.

[16] J. A. Morrison and M. J. Cross, "Scattering of a plane electromagnetic wave by axisymmetric raindrops," *Bell Syst. Tech. J.*, vol. 53, pp. 955–1019, 1974.

[17] V. A. Erma, "An exact solution for the scattering of electromagnetic waves from conductors of arbitrary shape: I. Case of cylindrical symmetry," *Phys. Rev.*, vol. 173, pp. 1243–1257, 1968.

[18] ——, "Exact solution for the scattering of electromagnetic waves from conductors of arbitrary shape. II. General case," *Phys. Rev.*, vol. 176, pp. 1544–1553, 1968.

[19] ——, "Exact solution for the scattering of electromagnetic waves from conductors of arbitrary shape. III. Obstacles with arbitrary electromagnetic properties," *Phys. Rev.*, vol. 179, pp. 1238–1246, 1969.

[20] H. R. Pruppacher and K. V. Beard, "A wind tunnel investigation of the internal circulation and shape of water drops falling at terminal velocity in air," *Quart. J. R. Met. Soc.*, vol. 96, pp. 247–256, 1970.

[21] H. R. Pruppacher and R. L. Pitter, "A semi-empirical determination of the shape of cloud and rain drops," *J. Atmos. Sci.*, vol. 28, pp. 86–94, 1971.

[22] S. Asano and G. Yamamoto, "Light scattering by a spheroidal particle," *Appl. Opt.*, vol. 14, pp. 29–49, 1975.

[23] C. Warner, "Effects of shape and orientation of spheroidal raindrops upon microwave scattering," *Electron. Lett.*, vol. 11, pp. 328–330, 1975.

[24] C. Warner and A. Hizal, "Scattering and depolarization of microwaves by spheroidal raindrops," *Radio Sci.*, vol. 11, pp. 921–930, 1976.

[25] A. R. Holt, N. K. Uzunoglu, and B. G. Evans, "An integral equation solution to the scattering of electromagnetic radiation by dielectric spheroids and ellipsoids," *IEEE Trans. Antennas Propagat.*, vol. AP-26, pp. 706–712, 1978.

[26] L. W. Li, P. S. Kooi, M. S. Leong, and T. S. Yeo, "On the simplified expression of realistic raindrop shapes," *Microwave Opt. Technol. Lett.*, vol. 7, no. 4, pp. 201–205, Mar. 1994.

[27] L. W. Li, P. S. Kooi, M. S. Leong, T. S. Yeo, and M. Z. Gao, "Microwave attenuation by realistically distorted raindrops: Part I—Theory," *IEEE Trans. Antennas Propagat.*, vol. 43, pp. 811–822, Aug. 1995.

[28] ——, "Microwave attenuation by realistically distorted raindrops: Part II—Predictions," *IEEE Trans. Antennas Propagat.*, vol. 43, pp. 823–828, Aug. 1995.

[29] Y.-L. Seow, "Computation on radar cross sections of dielectric spheroid: T-matrix approach," Master's thesis, Dept. Elect. Eng., National Univ. Singapore, 1997.

[30] J. O. Laws and D. A. Parsons, "The relation of raindrop-size to intensity," *Trans. Amer. Geophys. Union*, vol. 2, pp. 452–460, 1943.

[31] P. S. Ray, "Broadband complex refractive indices of ice and water," *Appl. Opt.*, vol. 11, pp. 1836–1844, 1972.

Yong-Lee Seow (S'97) received the B.Eng. degree (first-class honors) from the National University of Singapore, in 1997. He is currently working toward the M.Eng. degree at the same university.

Since 1997, he has been with the Department of Electrical Engineering, National University of Singapore as a Research Scholar. His current interest is in propagation and scattering of electromagnetic waves.

Le-Wei Li (S'91–M'92–SM'96), for a photograph and biography, see page 1748 of the December 1997 issue of this TRANSACTIONS.

Mook-Seng Leong (M'81), for a photograph and biography, see page 1748 of the Dcember 1997 issue of this TRANSACTIONS.

Pang-Shyan Kooi (M'75), for a photograph and biography, see the page 1748 of Dcember 1997 issue of this TRANSACTIONS.

Tat-Soon Yeo (M'80–SM'93), for a photograph and biography, see page 1748 of the December 1997 issue of this TRANSACTIONS.